







RESEARCH ARTICLE

10.1029/2022JG007328

Habitability of Polygonal Soils in the Hyper-Arid Atacama Desert After a Simulated Rain Experiment

Christof Sager¹ , Alessandro Airo^{1,2} , Kai Mangelsdorf³ , Felix L. Arens¹, Cornelia Karger³, and Dirk Schulze-Makuch^{1,4,5} 

Key Points:

- After simulating 20 mm rain on polygon and sand wedge, surface desiccated rapidly but in 10–15 cm depth soil was wet for at least 6 weeks
- Increased habitability was observed in the subsurface, which was more pronounced in the polygon compared to the sand wedge
- In addition to water availability, microbial abundance appears to be controlled by soil heterogeneities, that is, mineralogy and soil texture

Supporting Information:

Supporting Information may be found in the online version of this article.

Correspondence to:

C. Sager,
christof.sager@tu-berlin.de

Citation:

Sager, C., Airo, A., Mangelsdorf, K., Arens, F. L., Karger, C., & Schulze-Makuch, D. (2023). Habitability of polygonal soils in the hyper-arid Atacama Desert after a simulated rain experiment. *Journal of Geophysical Research: Biogeosciences*, 128, e2022JG007328. <https://doi.org/10.1029/2022JG007328>

Received 5 DEC 2022
Accepted 25 MAR 2023

Author Contributions:

Conceptualization: Christof Sager, Alessandro Airo
Data curation: Christof Sager, Kai Mangelsdorf, Cornelia Karger
Formal analysis: Christof Sager, Kai Mangelsdorf, Cornelia Karger
Funding acquisition: Christof Sager
Investigation: Christof Sager, Felix L. Arens
Methodology: Christof Sager, Kai Mangelsdorf, Felix L. Arens
Project Administration: Dirk Schulze-Makuch

¹Astrobiology Research Group, Zentrum für Astronomie und Astrophysik, Technische Universität Berlin, Berlin, Germany, ²Museum für Naturkunde, Leibniz-Institut für Evolutions- und Biodiversitätsforschung, Berlin, Germany, ³Section Organic Geochemistry, Helmholtz Centre Potsdam (GFZ) German Research Centre for Geosciences, Potsdam, Germany, ⁴Section Geomicrobiology, Helmholtz Centre Potsdam (GFZ) German Research Centre for Geosciences, Potsdam, Germany, ⁵Department of Experimental Limnology, Leibniz-Institute of Freshwater Ecology and Inland Fisheries (IGB), Stechlin, Germany

Abstract In the hyper-arid Atacama Desert, microbial life thrives near its “dry limit” in scarcely distributed habitats. Fracture networks of salt-poor sand wedges outlining salt-cemented polygons on alluvial surfaces in the Yungay region (Chile) represent potential microbial habitats. The degree of soil habitability at the surface (0–5 cm depth) and subsurface (10–15 cm depth) of a polygon and adjacent sand wedge was assessed before and up to 42 days after a 20 mm simulated rain experiment through the abundance of phospholipid fatty acids (PLFAs). Mineralogical composition, salinity, pH, electrical and thermal conductivity, water content, and water activity were analyzed for their relevance to habitability. After wetting, the PLFA content exclusively increased steadily with time in the polygon subsurface indicating the growth of an indigenous bacterial community. This increased habitability is presumably related to the soil's ability to retain water for at least 6 weeks at this depth. The lack of a continuous growth signal at the surface is likely due to rapid desiccation. In the sand wedge subsurface, the increase in PLFA content is not continuous despite the water activity being >0.9. The reason for this remains unclear but indicates that not only water availability is relevant for habitability but also the here described soil heterogeneities might impact the detection of the microbial response. Yet, the increasing PLFA trend in the polygon subsurface emphasized its relevance as a saline microbial habitat in an otherwise hostile environment, which could have implications for the assessment of soil habitability on Mars.

Plain Language Summary The limited water availability in the Atacama Desert challenges microbes which often occupy habitats that provide more water or more protected conditions than their surroundings. The extreme dryness led to fracture networks in the soils consisting of salt-poor sand wedges outlining salt-rich polygons representing major patterns of soil heterogeneity, and thus potential microbial habitats. A 20 mm rain was simulated to investigate their habitability (ability of the soil to support microbial activity), based on the content of phospholipid fatty acids (PLFAs). Mineral composition, pH, electrical and thermal conductivity, water activity and content were analyzed for their relevance to habitability. After moistening, continuously increasing PLFA abundances were monitored exclusively in the polygon subsurface, indicating enhanced habitability. We conclude that habitability is mainly controlled by water availability, which remained high for at least 6 weeks in the subsurface compared to the rapidly desiccating surface. Furthermore, habitability appears to be controlled by soil characteristics (i.e., soil heterogeneities), such as soil texture, type and content of salts which might explain low PLFA values in the sand wedge subsurface despite a high water availability. Our results emphasize the relevance of polygonal networks as microbial habitats in extreme environments, which could have implications for the Martian habitability.

1. Introduction

The hyper-arid Atacama Desert in northern Chile is one of the oldest and driest deserts on Earth, challenging the activity of microbial life due to extremely limited water availability, oxidizing conditions, high ultraviolet radiation, and high soil salinity (Houston & Hartley, 2003; Navarro-González et al., 2003). These harsh conditions result from the extreme aridity caused by the rain shadow effect of the pre-Cordillera and Andean mountains in eastern Chile and the cold Humboldt current along the Chilean coast, which creates an inversion layer largely preventing the formation of clouds (Houston & Hartley, 2003). Further, the Atacama Desert is bound by a

© 2023. The Authors.

This is an open access article under the terms of the [Creative Commons Attribution License](https://creativecommons.org/licenses/by/4.0/), which permits use, distribution and reproduction in any medium, provided the original work is properly cited.

Resources: Cornelia Karger
Supervision: Alessandro Airo, Dirk Schulze-Makuch
Validation: Felix L. Arens, Cornelia Karger, Dirk Schulze-Makuch
Visualization: Christof Sager
Writing – original draft: Christof Sager
Writing – review & editing: Christof Sager, Alessandro Airo, Kai Mangelsdorf, Felix L. Arens, Dirk Schulze-Makuch

Coastal Cordillera in the west, largely blocking moist air from the Pacific Ocean. However, moisture can partially migrate further inland through topographic corridors as fog. The position of the Atacama Desert in the subtropical high-pressure belt further intensifies the hyper-arid climate that has persisted for about 12 million years, interrupted by shorter and wetter periods (Jordan et al., 2014). The resulting low mean annual precipitation of less than 1 mm/yr in the hyper-arid core reduces erosion and leaching rates, which led to the massive accumulation of salts, particularly sulfates, nitrates and chlorides (Ewing et al., 2006; Houston, 2006). These unique environmental conditions in the Atacama Desert motivated extensive geological, climatological, and biological research, which is ongoing for more than 20 years, in which the Atacama Desert was established as a suitable Martian analog (Azua-Bustos et al., 2022; Navarro-González et al., 2003). Although initially described as lifeless and devoid of plants, highly adapted microbial life in the hyper-arid core region (e.g., Yungay) of the Atacama Desert thrives in particular habitats, some of which provide more moisture or more protected conditions than their surroundings, such as the pores of salt aggregates, below translucent rocks or sheltered beneath boulders (Davila et al., 2013; A. F. Davila & Schulze-Makuch, 2016; Hwang et al., 2021; Warren-Rhodes et al., 2006; Wierzbos et al., 2006). In addition to water availability, the habitability of certain microenvironments was hypothesized to be related to soil heterogeneities such as mineralogy or nutrient availability (Crits-Christoph et al., 2013; Kusch et al., 2020; Schulze-Makuch et al., 2021). In the Atacama Desert, environmental heterogeneities exist on a regional scale such as moisture gradients from the coast to inland, or North-South aridity gradients along which microbial diversity and abundance are reduced (Boy et al., 2022; Knief et al., 2020; Schulze-Makuch et al., 2018). In contrast, polygonal networks are a characteristic landscape-scale feature on alluvial surfaces in the Yungay region and display a particular form of more local soil heterogeneities. These fracture networks are characterized by salt-poor sand wedges outlining salt-rich polygons of several meters in diameter, forming extensive hexagonal and orthogonal patterns that have been proposed as environmental proxies for saline soils and hyper-arid conditions (Sager et al., 2021, 2022). In general, the upper meters of alluvial soils in the Yungay region are classified into locally termed soil horizons that can vary in depth, degree, and type of salt cementation (Erickson, 1981): The uppermost horizon is the *chusca*, a non-indurated gypsic horizon, underlain by the *costra*, an indurated gypsic horizon. The *caliche* located below the *costra* is a petrosalic horizon and is cemented by highly soluble salts such as nitrates and chlorides. The detailed formation of polygonal networks in these soils remains under debate but processes such as thermal contraction and/or de-/hydration of calcium sulfates were suggested to be involved (Ewing et al., 2006; Pfeiffer et al., 2021; Sager et al., 2021). Nevertheless, infrequent rain events play presumably an important role in the development of polygonal networks by transporting salts further down the soil profile, resulting in alluvial soil cementation and the observed salt sequences (Arens et al., 2021). To investigate the effects of heterogeneities in polygonal soil on habitability, following significant moisture input, we simulated a ~20 mm rain event on a polygon and its sand wedge in the Yungay region (24°04'33.7"S; 69°59'43.6"W), and characterized the physicochemical parameters and phospholipid fatty acid (PLFA) content of its surface and subsurface (Figure 1). PLFAs are a major component of bacterial membranes and are used as biomarkers indicative of viable bacterial communities. Hence, PLFAs can also be used as a proxy for soil habitability since their analysis can provide crucial information regarding the viability, abundance and diversity of bacterial communities and allows for a broad taxonomic evaluation (Connon et al., 2007; Harvey et al., 1986; Logemann et al., 2011; Mangelsdorf et al., 2019; White et al., 1979; Z. Zhang et al., 2017).

2. Materials and Methods

2.1. Field Work and Sampling

Sample collection and the simulated rain experiment took place during July and August 2019 in the Yungay region, 75 km southeast of Antofagasta in northern Chile (Figure 1). To simulate a ~20 mm rain event, 300 L of potable water was evenly distributed on a confined part of a polygon and its corresponding sand wedge (24°04'33.7"S, 69°59'43.6"W) during sunset on 28 July 2019 (Figures 1, Figure 2). Samples were collected from the polygon and sand wedge in two depth ranges (surface 0–5 cm and subsurface 10–15 cm) using a sterile spoon while wearing gloves and masks yielding four samples per sampling time. Samples were collected at the following time points: one day prior to the simulated rain event (dry conditions), immediately following wetting (within 20 min, here referred to as “direct” or “directly after”), as well as 1, 7, 14, and 42 days thereafter. For the different days, samples were taken at adjacent soil positions. At each time point and soil unit, five sample aliquots (1 × plastic bag, 2 × 50 mL glass container, 2 × 50 mL polypropylene tubes) were collected from a 15 × 15 cm sampling area in which the sediment was homogenized with a sterile spoon to reduce the effects of soil heterogeneities within

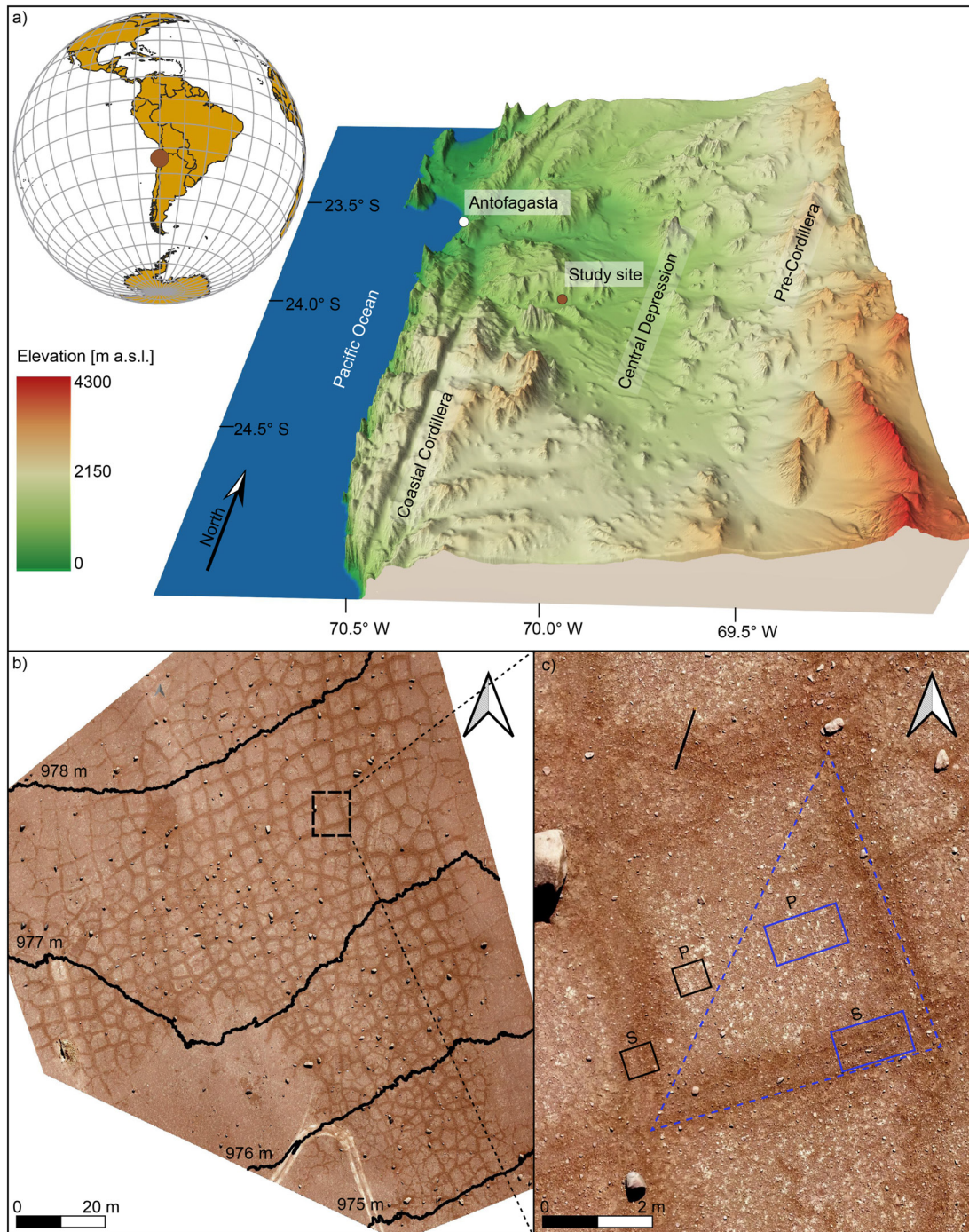


Figure 1. Location maps of the study area. (a) The location of the study site ($24^{\circ}04'33.7''\text{S}$, $69^{\circ}59'43.6''\text{W}$) is shown on a globe map and as a 10 \times vertically exaggerated 3D model on the eastern margin of the Coastal Cordillera, near the city of Antofagasta. (b) An orthophoto of the polygonal network, and (c) a close-up orthophoto of the polygon (P) and corresponding sand wedge (S) on which the rain experiment was conducted with the indicated wetting area (blue dashed triangle), sampling areas before (black rectangles) and after the simulated rain event (blue rectangles); modified from Sager et al. (2021).

the respective soil samples. Aliquots used for salt content and mineralogy analysis (~ 300 g) were stored at room temperature, the aliquots for water activity and water content were stored at 4°C and for PLFA analysis (15–60 g) at -20°C . Water activity depends on the prevailing temperature that exhibits daily and seasonal variations in the study area. Here, samples were collected during the late afternoon when daily air temperatures were among the highest and water activity and content were among the lowest. Thermal conductivity and temperature of surface

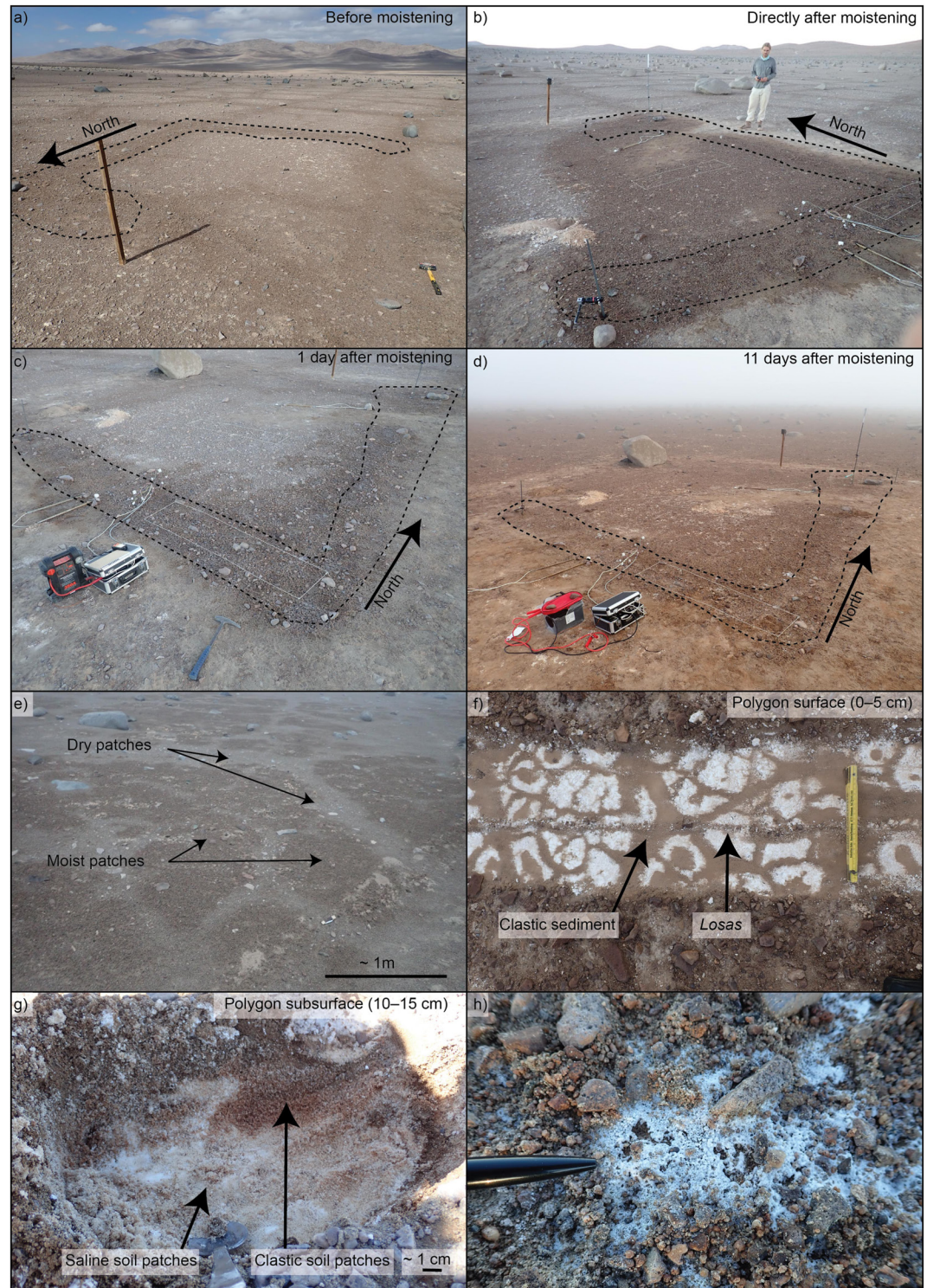


Figure 2. Field photos showing the polygon and sand wedge (dashed lines represent wetted parts of the sand wedge) before (a), directly after (b), 1 day after (c), and 11 days after the simulated rain when a natural fog event re-wetted the surface (d). Moist and dry patches during a fog event in the vicinity of the study area presumably resemble polygons and their sand wedges (e). Removal of the sediment surface layer reveals soil heterogeneity: white sulfate aggregates, locally referred to as *losas* embedded in more clastic and salt-poor brown soil patches (f). Similarly, the vesicular polygon subsurface contains saline and more clastic soil patches, which were sampled separately on day 7 (g). After 7 days salt efflorescence appeared on the surface of the sand wedge (h).

sediments were recorded for the polygon and sand wedge surface at a depth of about 5 cm before moistening as well as directly after (within 20 min), 1 day and 5 days after moistening using the thermal properties analyzer *KD2Pro* (Decagon Devices, Inc). Further, the soil temperature and relative humidity were recorded during the experiment using data loggers (Onset Hobo pro v2) at depths of 10, 35, and 50 cm for the polygon and sand wedge as previously reported by Sager et al. (2021).

2.2. Analysis of Soil Characteristics

X-ray diffraction (XRD) was performed on all samples to identify the mineralogical composition using a Bruker D2 Phaser benchtop diffractometer with Cu radiation and a Ni filter at the Department of Applied Geochemistry at Technische Universität Berlin. A semi-quantitative XRD analysis (SQ-XRD) was carried out using the “Diffrac.eva” software and the “Powder Diffraction File Minerals 2019” (database of the *international centre for diffraction data*). Prior to analysis, the samples were dried at 40°C and crushed to a fine powder using a XRD McCrone mill. Samples were scanned between 3° ($2\theta = 2\theta$) and 80° (2θ) at 30 kV and 10 mA using a step size of 0.1° (2θ) and a count time of 2 s. Scan time was about 70 min with a 1 mm divergence slit, and 1 mm air scattering screen. Additionally, the salt content of the samples, also referred to as the soil salinity, was determined by complete leaching with distilled water. Therefore, the powdered samples (3–5 g) from XRD analysis were weighed prior to and after leaching; the weight difference being equivalent to the salt content in weight percent (wt%). The water content of sediment samples was gravimetrically determined by drying samples at 40°C and using the difference in weight of samples before and after drying.

The water activity is defined as the ratio of vapor pressure of water in a sample solution to pure water at similar conditions and expressed by the a_w -value which ranges from zero to one (i.e., water activity of pure distilled water). It is a measure of available water for microbial growth and was measured with the *Labmaster-aw Neo* water activity probe (Novasina AG), using a stability observation time of 15 min, during which the a_w -value did not change more than 0.001 units within 15 min. Samples that reached a_w -values >1 ($a_{w\max} = 1.0162$), were interpreted to be 1, as $a_w > 1$ is a result of measurement uncertainty. For soil pH measurements, 5 g of dried soil (<2 mm) was dispensed in 12.5 mL distilled water and put on a vibrating table for 30 min and measured using the HQ40D Portables 2-Canal Multimeter (Hach Company). The electrical conductivity was measured using the GMH 3400 Series conductivity measuring device (GHM Messtechnik GmbH) after dispensing 5 g of dried soil (<2 mm) in 25 mL distilled water and placing it on a shaking table for 60 min.

2.3. Phospholipid Fatty Acid (PLFA)—Extraction and Column Separation

In total 20 samples of approximately 30–60 g of freeze-stored soil were collected for PLFA analysis from the two depth ranges of the polygon and sand wedge before moistening, and 1, 7, 14, and 42 days thereafter. These samples were dried in an oven at 35°C for a maximum of 2 hr before grinding using a rotating disc mill. Extraction from ground samples was performed using a flow bending system for 5 minutes with an extraction solvent mixture of methanol, dichloromethane (DCM), ammonium acetate buffer at a ratio of 2:1:0.8 (v/v) (Bligh & Dyer, 1959) and at a pH of 7.6. The solvent solution was centrifuged for 10 min at 2,500 rpm to separate the sediment from the extract. The soil material was re-extracted twice with DCM and all extracts were combined in a separation funnel. Afterward, an internal standard (PC_{D54} , deuterated phosphatidyl choline) for compound quantification was added. The organic phase was separated from the water phase by changing the solvent mixture ratio to 1:1:0.9 (v/v). The organic phase was separated, and the water phase was re-extracted twice with DCM. All organic phases were combined and the solvent was evaporated to dryness using a *TurboVap 500* and finally a gentle stream of nitrogen (Zink & Mangelsdorf, 2004). Subsequently, the organic extracts were separated by chromatographic column separation into a low-polar lipid, free fatty acid, glycolipid, and phospholipid fraction by using two columns in sequence: an upper column filled with 1 g silica gel (63–200 μ m) and 0.5 g sodium sulfate on top and a lower column filled with 1 g Florisil (150–250 μ m). The low-polar lipids were eluted with 20 mL chloroform, the free fatty acids with 50 mL methyl-formate with 0.025% glacial acetic acid and the glycolipids with 20 mL acetone. The phospholipids were extracted only from the silica gel column with 25 mL methanol. To improve the phospholipid recovery the column material was re-extracted with a methanol-water mixture (1:0.6). For phase separation the above-mentioned ratio of 1:1:0.9 (dichloromethane, methanol, water) was adjusted in a separation funnel and the organic phase was combined with the phospholipid fraction. The collected fractions were concentrated to dryness in a *TurboVap 500* and finally under a gentle stream of nitrogen.

2.4. Phospholipid Fatty Acid (PLFA)—Detection of PLFA

For the phospholipid fatty acid analysis, the phospholipid fraction was exposed to an ester cleavage procedure described by Müller et al. (1990) where the phospholipid linked fatty acid esters are directly transformed into their respective fatty acid methyl esters (PLFAs) using trimethylsulfonium hydroxide. Subsequently, the PLFAs were measured on a Trace Gas Chromatograph 1310 (Thermo Scientific) coupled to a TSQ 9000 mass spectrometer (Thermo Scientific). The gas chromatograph was equipped with a cold injection system operating in the splitless mode and a SGE BPX 5 fused-silica capillary column (50 m length, 0.22 mm ID, 0.25 μm film thickness) using the following temperature conditions: initial temperature 50°C (1 min isothermal), heating rate 3°C/minute to 310°C, held isothermally for 30 min. Helium was used as carrier gas with a constant flow of 1 mL/min. The injector temperature was programmed from 50° to 300°C at a rate of 10°C/s. The MS operated in the electron impact mode at 70 eV. Full-scan mass spectra were recorded from m/z 50 to 650 at a scan rate of 1.5 scans/s. The PLFA abundance is given as a weight fraction, that is, as nanogram PLFAs per gram sediment (ng/g).

2.5. Statistical Analysis

A principal component analysis (PCA) was conducted to reduce the linear dimensionality of the used data set by singular value decomposition of the data using the *Scikit-learn Python* module (Pedregosa et al., 2011). The results were plotted in a scree plot showing the explained variance of the principal components (PC) including the loading scores for PC1 and PC2. Additionally, a two-dimensional PCA biplot shows the clustering of samples along PC1 and PC2. A two-sample unpaired *t*-test was conducted using the *t*-test function in Microsoft Excel to test if the number of different PLFAs between the surface and subsurface varies significantly between each other.

3. Results

3.1. Geological Characterization of the Sampling Site

The investigated polygon and surrounding sand wedge have an area of $\sim 30 \text{ m}^2$, a perimeter of $\sim 22 \text{ m}$ and are located at an elevation of $\sim 1,000 \text{ m a.s.l.}$ in the center of a polygonal network that developed in alluvial sediments (Figures 1, Figure 2). The mineralogical composition of the insoluble fraction of all four soil units (surface and subsurface of polygon and sand wedge) is dominated by feldspars and quartz with small amounts of amphiboles and occasionally phyllosilicates (Figure 3). Note that the salt content determined by weight loss after sample leaching (in weight percent, Figure S1 in Supporting Information S1) and by SQ-XRD (in percent, Figure 3) differs. However, trends between the two methods are similar and comparability between samples and soil units is maintained. The major difference between the polygon and the sand wedge is the salt content, which is low in the sand wedge and high in the sulfate-cemented polygon (Figure 3, Figure S1 in Supporting Information S1). In particular, the polygon surface (0–5 cm) with a mean salt content of 31 wt% (standard deviation = 2.3 wt%) contains palm-sized aggregates composed of CaSO_4 in different hydration states that is, gypsum ($\text{CaSO}_4 \cdot 2\text{H}_2\text{O}$), anhydrite (CaSO_4) and bassanite ($\text{CaSO}_4 \cdot 0.5\text{H}_2\text{O}$), which are common for the upper *chusca* horizon (Figure 2f, Figure 3, Figure S1 in Supporting Information S1) (Diaz, 1994; Ericksen, 1983). These calcium sulfate aggregates are locally referred to as *losas* and submerged in loose clastic sediments. The wetting by the rain experiment did not lead to major changes in the salinity of the polygon surface (Figure S1 in Supporting Information S1). However, changes in mineralogy were observed, such as the detection of gypsum only after wetting, while after day 1 a mixture of varying amounts of gypsum and anhydrite were present. In contrast, the polygon subsurface lacks the *losas* but exhibits a vesicular texture of more clastic and saline soil patches, which is typical for the lower *chusca* horizon (Figure 2g). These soil patches contain locally varying amounts of gypsum (mean salt content of 50 wt%, standard deviation = 16.5 wt%) throughout the experiment, while no changes in mineralogy after the rain event were observed. This heterogeneity in the gypsum distribution is illustrated by two additional samples collected on day 7, including a clastic soil patch with a salt content of 16 wt% and a saline soil patch with 78 wt% (Figure 3c, Figure S1 in Supporting Information S1). The sand wedge surface initially contained minor amounts of highly soluble halite and nitratine, being absent directly after wetting and 1 day thereafter, indicating the downward leaching of these salts. Irregularly distributed salt efflorescence was observed in the field on the sand wedge surface 7–14 days after wetting and detected by XRD, suggesting an upward migration of brines and their subsequent evaporation (Figure 2h, Figure 3). However, at day 42, soluble salts were not detected with XRD analysis but with total salt content analysis using sample leaching (Figure 3, Figure S1 in Supporting

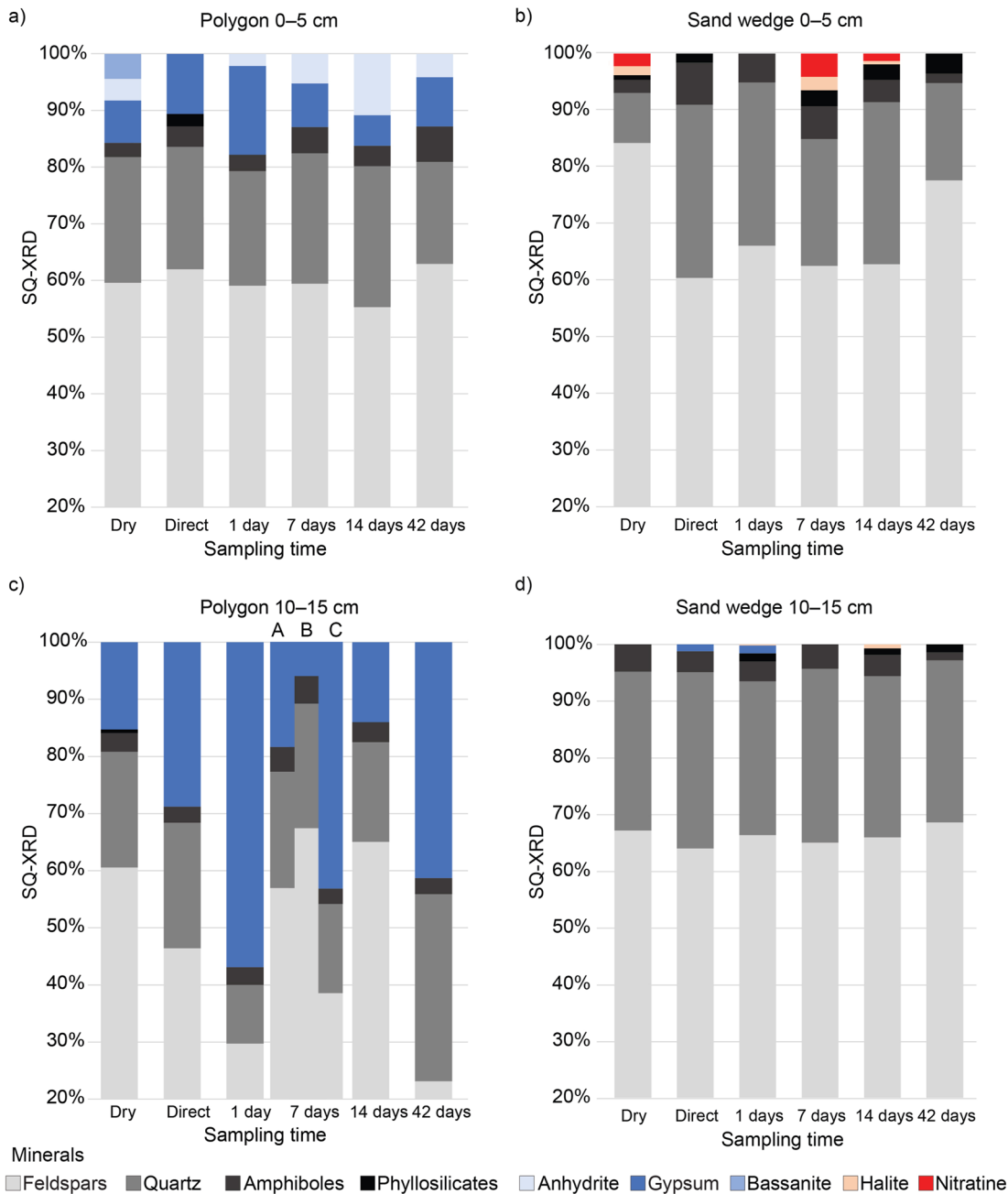


Figure 3. Mineralogical composition of the investigated soil units revealed by semi-quantitative X-ray diffraction (SQ-XRD) analysis of the surface and subsurface samples of the polygon (a,c) and the sand wedge (b,d) along the course of the experiment. On day 7, three samples were collected for the polygon unit in 10–15 cm depth including a pooled sample (A), clastic soil patch with a brown color (B) and saline soil patch of white color (C) to illustrate soil heterogeneity.

Information S1). The composition of the sand wedge subsurface is dominated by the aforementioned insoluble minerals but minor amounts of gypsum were detected directly after and 1 day after wetting, while halite was detected 1 and 14 days after wetting (Figure 3). The electrical conductivity decreases in all soil units after moistening and increased at the sand wedge surface by day 7, further supporting the primary downward transport of soluble minerals, followed by upward migration of brines toward the sand wedge surface (Figure 2h, Figure S2 in Supporting Information S1). The largest differences in soil pH are between sand wedge units with a mean pH of 8.6 and the slightly less alkaline polygon units with a mean pH of 7.8 (Figure S2 in Supporting Information S1). After wetting, no major pH shifts were observed, except for the sand wedge subsurface. There, the pH decreased slightly in the first 24 hr to ~8, increased to 9.5 by day 14 and fell back to 8.7. Similarly, the conductivity varied

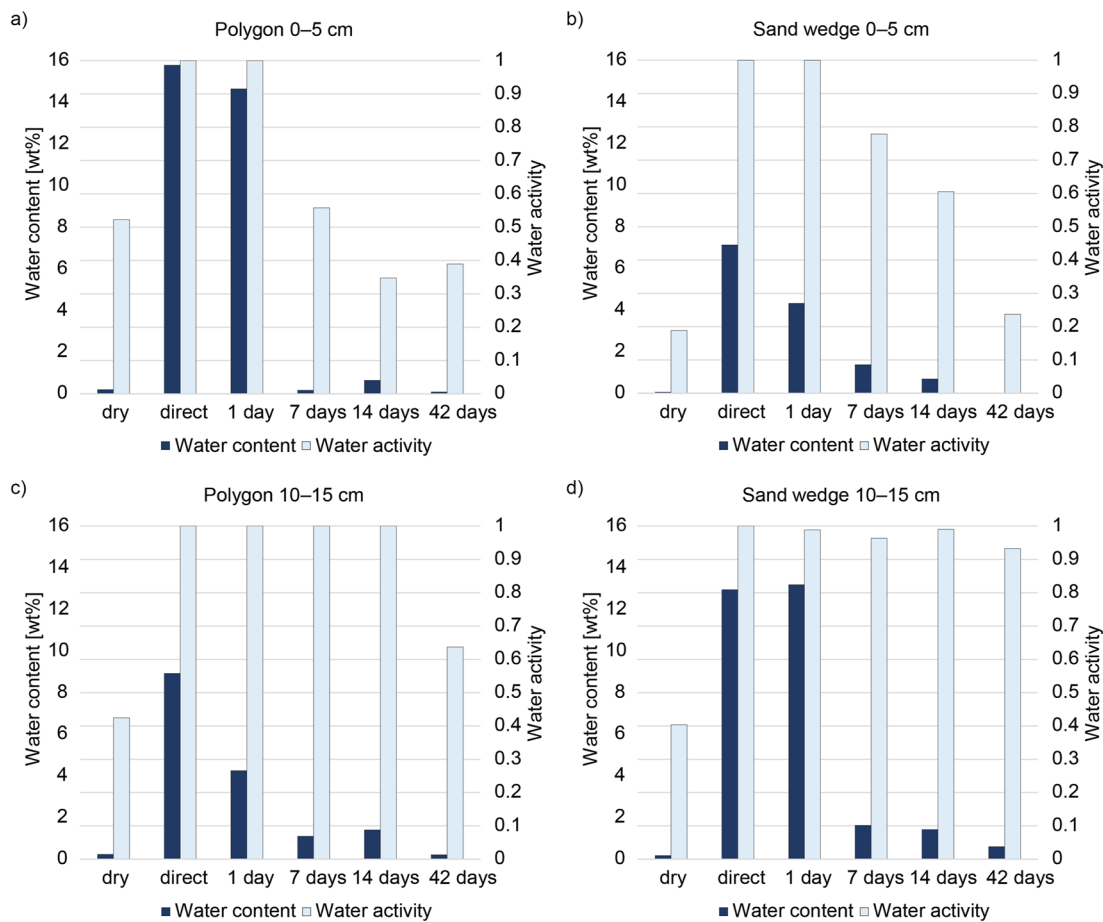


Figure 4. Water content and water activity measurements for the surface and subsurface samples of the polygon (a, c) and the sand wedge (b, d). Water activity is expressed by the a_w -value, which is the quotient of the water vapor pressure of a sample and that of pure water under the same conditions.

between the sand wedge with a higher mean thermal conductivity ($0.44 \text{ W/m} \times \text{K}$) compared to the polygon ($0.12 \text{ W/m} \times \text{K}$) (Figure S3 in Supporting Information S1). The polygon had slightly higher surface temperatures compared to the sand wedge, while below the surface, from 10 cm depth on, the polygon remained colder (e.g., 1.5°C on average at 10 cm) than the sand wedge (Figure S3 in Supporting Information S1).

3.2. Water Availability

The availability of water is critical for soil habitability and compared to the water content, the water activity is a more relevant factor as it is considered a measure of the freely available water for microbial life. The threshold of water activity required to support microbial growth varies between species, but higher water activities generally support the growth of more microorganisms. The lowest water activity under which cell division was observed is 0.585 for the fungal halophile/xerophile *Aspergillus penicillioide* (Stevenson et al., 2017). It was also reported that some deep-sea sulfate reducers may thrive down to a water activity of ~ 0.4 (Steinle et al., 2018). Prior to the rain experiment, the water content in all soil units was low with values below 0.2 wt% (Figure 4). The water activities in the polygon ranged between 0.51 at the surface and 0.42 in the subsurface. In the sand wedge, water activity was even lower ranging from 0.19 at the surface to 0.40 in the subsurface. Directly after moistening, an increased water content and water activity of ~ 1.0 were observed in all soil units. Water activities and contents remained relatively similar by day 1 but the surface units started to desiccate between days 1 and 7, reaching values similar to the dry conditions by the end of the experiment. One day after moistening, the first centimeters of the polygon surface already appeared dried out compared to the sand wedge (Figure 2c). However, below the first centimeters of sediment, the polygonal soil remained moist, resulting in an overall higher water content than in the sand wedge surface at day 1 (Figure 4). A fog event occurred 11 days after moistening at which the pristine

soil surfaces appeared re-wetted (Figure 2d). A similar observation was made in the vicinity of the experimental area, where moist polygonal patches were surrounded by linear dry patches, potentially representing polygons that contained hygroscopic salt and salt-poor sand wedges (Figure 2e). By day 14, the polygon surface had a lower water activity than the sand wedge surface, although it had a similar water content, which may result from hygroscopic salts such as anhydrite affecting the water activity (Davila et al., 2013; Lebron et al., 2009). In contrast to the surface, the subsurface of the polygon ($a_w = 0.64$, water content = 0.2 wt%) and the sand wedge ($a_w = 0.93$, water content = 0.6 wt%) desiccated less rapidly and had greater water activities and contents until the end of the experiment.

3.3. Phospholipid Fatty Acid Analysis

PLFAs were found in all surface and subsurface samples of the polygon and sand wedge at concentrations ranging from 4 to 122 ng/g (Figure 5). These are overall very low PLFA concentrations especially in the sand wedge subsurface at day 1 which is with 4 ng/g in the range of the blank values. At initial dry conditions, the polygon surface exhibited the highest PLFA abundance of all soil units. After wetting, PLFA abundance in the polygon surface initially remained almost constant at day 1 but decreased to lower levels between days 7 and 42. In contrast, the PLFA values in the subsurface of the polygon increased continuously throughout the entire experiment reaching their highest value at day 42. The sand wedge exhibited similarly low PLFA abundances in the surface and subsurface at initial dry conditions. Wetting resulted in an initial large PLFA increase at the sand wedge surface to 122 ng/g on day 1 while in the subsurface the PLFA abundance remained low. In the further course of the experiment, the PLFA values of the sand wedge surface decreased to similar levels as during dry conditions. In contrast, the PLFA abundances in the sand wedge subsurface increased from day 1 to day 14 but decreased already at the end of the experiment to values similar to the initial dry conditions. The comparatively low PLFA diversity does not change significantly for each soil unit throughout the field experiment and ranges from 5 to 16 different PLFAs but is significantly higher (two-sample *t*-test, *p*-value = 0.0005) in the surface units (mean = 13) compared to the subsurface units (mean = 9). The PLFA inventories of all soil units are dominated by the taxonomically not specific normal saturated fatty acids in the range from C₁₄ to C₂₄ with an average relative abundance (RA) of 67%. They are followed by monoenoic fatty acids (RA = 26%) with 16, 17 and 18 carbon atoms being indicative for Proteobacteria and by polyenoic fatty acids (RA = 5%) which could either derive from eukaryotic and/or bacterial biomass. In contrast to these PLFA groups, which are found in all samples, terminally branched saturated *iso*- and/or *anteiso*-fatty acids with 15, 16, 17, and 18 C-atoms indicative of firmicutes, cyclopropyl fatty acids (RA = 0.8%) with 17 C-atoms and mid-chain branched 12-methyl palmitic acid (RA = 0.1%) indicative for *Rubrobacter* (Suzuki et al., 1988), are only present in minor RA and not in all samples (Figure S4 in Supporting Information S1). For example, the mid-chain branched saturated fatty acids occur only in surface samples after day 14 (Figure S4 in Supporting Information S1). The predominance of saturated PLFAs can be an indication that the microbial communities are adapted to warm environmental conditions, since cell membranes with a high proportion of saturated FAs show higher phase transition temperatures (membrane melting temperature), which is favorable to keep the membrane in an adequate fluid stage at warm ambient temperature (Suutari & Laakso, 1994). Pure phospholipid ethers indicative of viable *Halobacteria* (*haloarchaea*) were surprisingly not detected in any sample. However, phospholipids combining ether and fatty acid side chains were found. Overall, due to the low diversity of PLFAs compared to normal soils the content of further taxonomic information is rather restricted.

3.4. Statistical Analyses

A principal component analysis (PCA) was applied to display relationships between samples and to infer the influence of environmental and biological parameters that explain the largest variance in the data set. The PCA shows that the first two principal components explain a relatively low total variation of 40.3% (Figure 6). Yet, a clustering of four groups, each representing samples from one soil unit can be observed in the PCA biplot, indicating correlation between samples of each soil unit. Further, the PCA also differentiates pairs of soil units, that is, between the polygon units and the sand wedge units along PC1; and between the subsurface- versus the surface units along PC2. The separation of polygon and sand wedge samples along PC1 is best explained by high loadings in the salt (loading score = 0.37), gypsum (loading score = 0.34) and polyenoic PLFA content (loading score = 0.31). The separation of surface and subsurface cluster along PC2 is best explained by sampling depth,

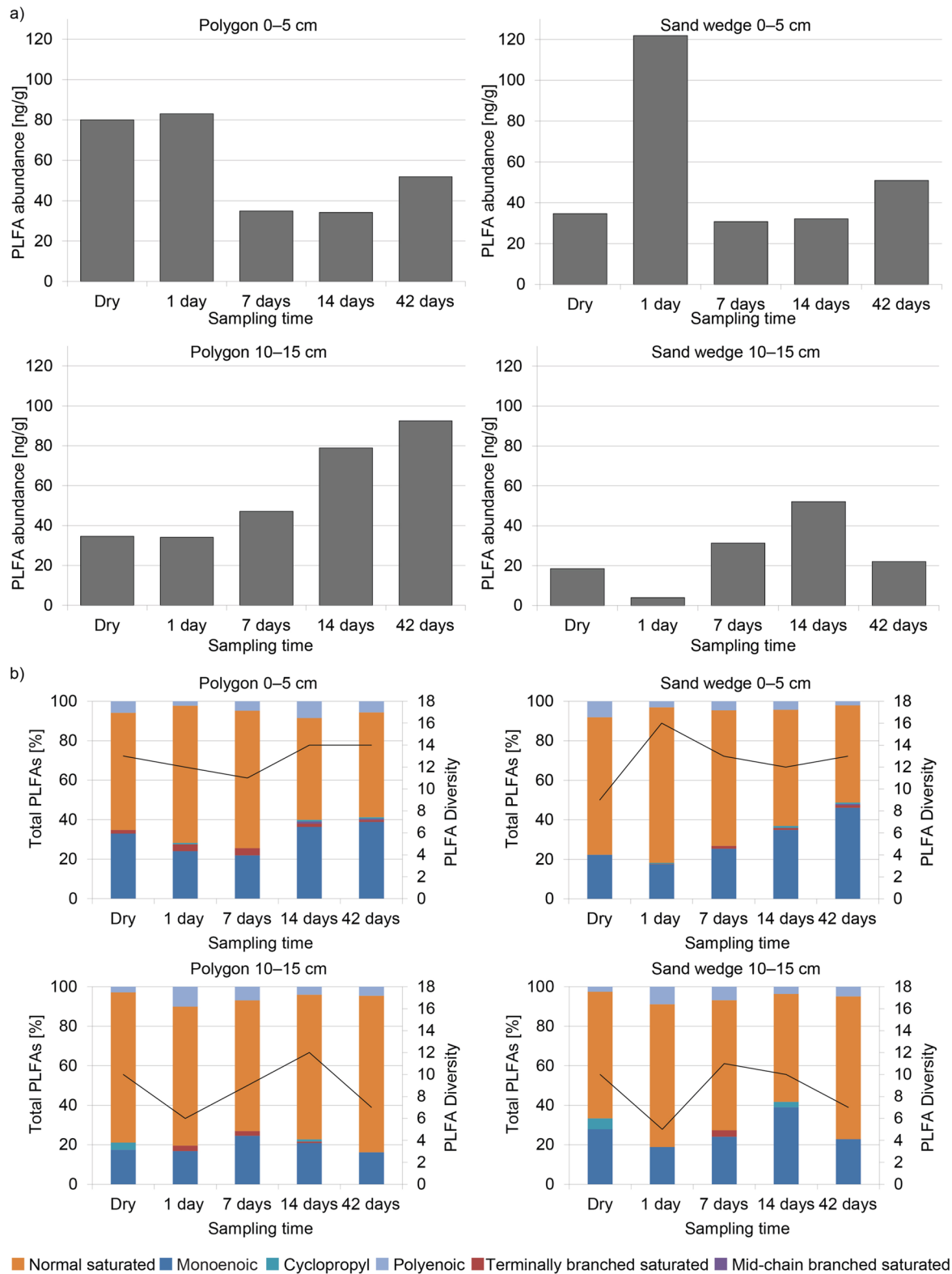


Figure 5. Results of phospholipid fatty acid (PLFA) analysis. (a) Absolute PLFA abundances in nanogram per gram sediment in the four soil units. (b) The relative abundance of PLFA structural groups displayed as color-coded bar columns and the number of PLFAs displayed as a black line.

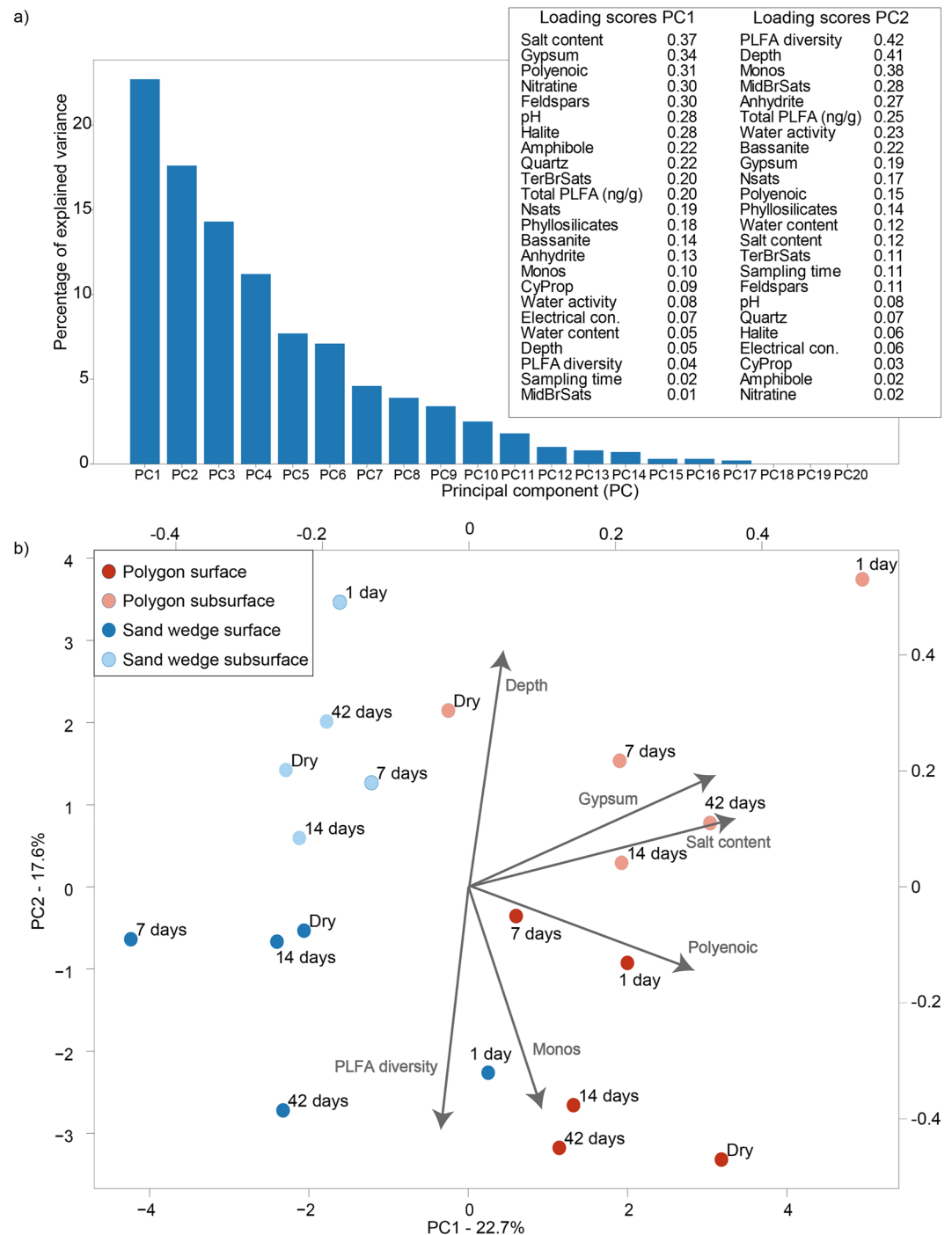


Figure 6. Principal component analysis (PCA) of all samples and measured parameters. (a) Scree plot showing the explained variance of the principal components (PC) with the loading scores for PC1 and PC2. Loading scores are shown for sampling depth (depth), sampling time (time), water content, water activity, salt content, pH, minerals as well as for the total phospholipid fatty acid (PLFA) abundance, the PLFA diversity and structural fatty acid features including monoenoic (Monos), cyclopropyl (CyProp), mid-chain branched saturated (MidBrSats), terminally branched saturated (TerBrSats), normal saturated (Nsats) and polyenoic FAs. (b) The PCA biplot of color-coded samples with their sampling time and gray arrows representing the parameters with the highest loadings for PC1 (salt content), gypsum content (gypsum), polyenoic fatty acids, and PC2 (PLFA diversity, depth, and monoenoic fatty acids). The numbers next to the axis label are the percentage of explained variance of the respective PC.

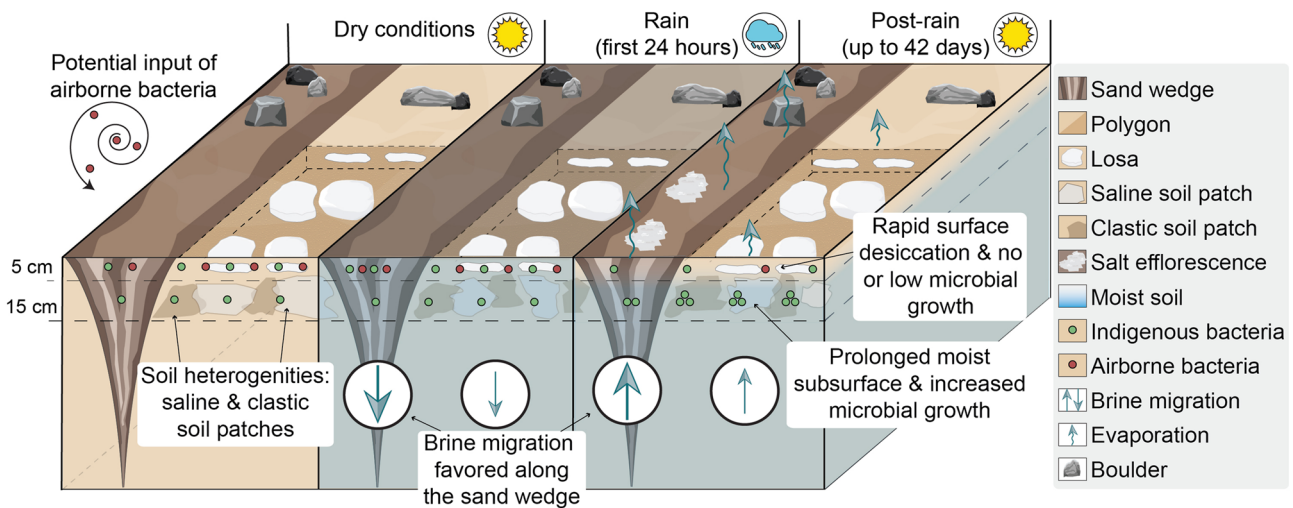


Figure 7. Conceptual interpretation of the processes in the polygon and sand wedge system before, during, and after a rain event based on the measured environmental parameters and microbial membrane lipid analysis. The polygon and sand wedge display local soil heterogeneities, while *losas* and saline soil patches within more clastic sediment represent intra-polygon heterogeneities. Under dry conditions, a mixture of indigenous and airborne microbes introduced by wind reside in the surface layer of the polygon and sand wedge. The rain moistens the soil and transports salts and water down the soil profile, especially along the more permeable sand wedge. Ongoing moist conditions for at least 42 days in the subsurface allow for microbial growth, especially in the polygon and in part in the sand wedge. In contrast, the surface soil of the polygon and sand wedge desiccates rapidly leading to low or no microbial growth in the post-rain period.

(loading score = 0.41) which is not surprising, and by the number of PLFAs further supporting the *t*-test results (loading score = 0.42) and monoenoic fatty acids (loading score = 0.38). Further, the water content and water activity explain the cluster separation between the surface and subsurface units with loadings of 0.12 and 0.23, respectively (Figure 6).

4. Discussion

Our results, supported by statistical analyses, show that the four soil units vary from each other regarding composition, soil texture, pH, electrical conductivity, thermal conductivity, temperature, and water availability. Furthermore, the soil units responded differently to the simulated rain event, especially regarding water and brine migration and, more importantly, their habitable conditions based on PLFA abundances and trends.

Overall, the detection of PLFAs in all soil units prior to wetting, albeit in low amounts, indicates that microbial life is present in the polygon and adjacent sand wedge. The relatively low number of different PLFAs suggests a low diversity of the microbial community in all soil units, which might reflect the extreme environmental conditions in the Atacama Desert close to the dry limit for life. The rain experiment led to an increase in water activity from values below 0.6 to ~1.0 in all soil units by day 1, providing conditions suitable for microbial growth. Yet, at day 1, the PLFA content in the polygon surface remained at similar levels whereas at the sand wedge surface, the PLFA content was greatly increased, indicating a rapid but short stimulation of the microbial community in the sand wedge surface. However, a trend of decreasing PLFA abundances in both surface units to values below and similar to the initial dry conditions suggests an overall decrease in habitability following the first 24 hr (Figure 7). This trend is accompanied by a decreasing water activity in the surface units due to rapid surface desiccation after day 1. In contrast, the water activities in the subsurface units at a depth of 10–15 cm remained in the habitable regime, that is, >0.6, throughout the experiment. These moist conditions are associated with steadily increasing PLFA abundances in the polygon subsurface, which resulted in the highest PLFA value at day 42, suggesting improved habitability conditions due to high water availability. In the sand wedge subsurface, a similar but less clear and less significant trend of increasing PLFA abundances can be observed, which unexpectedly decreased again by day 42 despite a high water activity of >0.9. Thus, we assume that detected variations in the measured biological and physicochemical parameters partially reflect the heterogenous nature of these soils resulting from aridity-driven soil processes in the Atacama Desert. At the same time, certain variations in these parameters, such as the electrical conductivity, water content and water activity, can be interpreted, to be a direct result of the here applied moisture input, while for example, variation in gypsum content in the polygon subsurface is likely

due to the saline and clastic soil patches. Thus, the question remains how much of the PLFA variation is due to the induced wetting of the soils and what is related to spatial soil heterogeneity. In the polygon subsurface, the steadily increasing PLFA abundance provides good indication that the subsurface microbial community is indeed stimulated by the wetting of the soil. In the sand wedge subsurface, such stimulation appears to be less pronounced and does not correlate well with the water activity ($R^2 = 0.06$), but does correlate well with for example, the pH value ($R^2 = 0.89$) suggesting that natural heterogeneities of the physical soil characteristics may play a greater role in causing higher variability of the PLFA signal. Such soil heterogeneities could explain the higher PLFA abundance despite a lower water activity in the polygon compared to the sand wedge at day 42. Alternatively, it is conceivable that the preferred migration of brines along the sand wedges due to a higher permeability than in the salt-cemented polygon creates more salt stress to the microbial community compared to the polygon. This is indicated by the patchy formation of salt efflorescence on the wedge surface and a higher standard deviation of the electrical conductivity in the sand wedge (SD: 2.9 mS) than in the polygon (SD: 0.39 mS) suggesting less stable saline conditions within the two sand wedge units. Similarly, the patchy formation of salt efflorescence suggests that brine migration within the sand wedge is also not homogeneous. Given rare rain events, such brine migration would be cyclic over longer time periods and could explain the reported minimal cementation of sand wedges in the vicinity (Sager et al., 2021), but also contribute to the reported major cementation of sulfate wedges north of the study area (Zinelabedin et al., 2022). Both subsurface units remained moist throughout the experiment, and it remains unclear if either the soil column of the polygon or sand wedge dries out more quickly, but the presence of hygroscopic salts and cementing sulfates that reduce permeability in the polygons suggest, that ultimately the polygons have a higher water retention potential than the sand wedges. Furthermore, it can be speculated whether the higher content of crystal water contained in gypsum in the polygon might be advantageous for sustaining habitability over longer periods. The absence of anhydrite and bassanite in the polygon surface after wetting might indicate such hydration processes but it could similarly be a result of the natural variability in the soils, especially since anhydrite was detected in the samples collected between days 1 and 42. However, the relevance of crystal water for example, in gypsum as a water source for microbes remains highly debated (Huang et al., 2020; Wierzechos et al., 2020), and would here at most be relevant for prolonged dry conditions. Similarly, moisture provided by fog and dew events might be better adsorbed by the anhydrite- and bassanite-rich surface soils of the polygon compared to the sand wedge, lacking such hygroscopic minerals (Figures 2c and 2e, Figure 3), but it remains unclear whether this improves the habitability of the polygon surface during dry conditions, as the higher PLFA concentrations might suggest (Figure 5). Furthermore, the microporous nature of calcium-sulfate aggregates or crusts has been suggested to absorb moisture during periods of high relative humidity (Wierzechos et al., 2011). Thus, given the component of natural variability due to soil heterogeneities, we can only relate the increasing PLFA contents in the polygon subsurface to an overall increased habitability and stimulation of a local microbial community that is presumably adapted to the predominating dry and saline conditions under which it thrives. In contrast, the reduced PLFA contents and thus reduced microbial abundance at the surface after day 1 presumably do not relate to an extended period of increased habitability. However, the PLFA spike at the surface at day 1 after wetting stands out from the overall PLFA patterns. A rapid response of the surface microbial community might be plausible since survival strategies in extreme desert environments might include a rapid response with respect to transient moisture input. However, such a spike is not observable in the polygon surface sample, which could indicate that the PLFA spike in the sand wedge sample might also be influenced by soil variabilities. Nevertheless, it is an interesting thought that the microbial community at the surface reacts differently than that of the subsurface as indicated by the slow and steady increase of microbial abundance in the polygon subsurface, where the microbial community is protected from direct desiccation and UV-radiation and where enhanced habitable conditions, therefore, might persist longer. Due to the restricted PLFA inventory, it remains difficult to identify small variations in the microbial communities against the background of natural soil heterogeneities (Figure S4 in Supporting Information S1). However, such variations might be indicated, for example, by the presence of mid-chain branched saturated fatty acids, which occur only in the surface units after day 14 (Figure S4f in Supporting Information S1). Additionally, it is also conceivable that variations in PLFA contents are partially influenced by the migration of bacterial populations following the water movement during the simulated rain or subsequent evaporation.

In this study, we highlight that variations in PLFA abundances contain a component reflecting the heterogeneous distribution of microbial populations due to the here described soil heterogeneities. This corroborates the findings of previous studies conducted in the Atacama Desert (Crits-Christoph et al., 2013; Kusch et al., 2020) as well as locations in Europe and Australia that emphasized that variations in soil characteristics impact the

diversity or abundance of microbial life (Carson et al., 2009; Certini et al., 2004). We found in our study that physicochemical soil parameters not only vary with depths but also contain a significant lateral diversity, primarily displayed by polygons and sand wedges (Figure 7). Furthermore, soil heterogeneities exist within single soil units, for example, clastic and saline soil patches in the polygon subsurface, *losas* within clastic sediment in the polygon surface or patchy salt efflorescence on the sand wedge surface (Figure 7), while overall environmental conditions, such as elevation, air temperature and air relative humidity remain similar between neighbored polygons and sand wedges. Thus, we conclude that variations in soil habitability in the study area are mainly due to differences in water availability but are also controlled by soil heterogeneities, such as soil composition and soil texture. Based on this study we suggest that sampling strategies must be adapted to the degree of soil heterogeneity to distinguish biological signals due to the induced moisture input from signals due to the natural variability of the soil. To reduce the effect of natural variability on single data points, in future studies more replicates have to be collected in a spatially random manner instead of sampling just at adjacent soil positions. However, since underlying soil heterogeneities are often not detectable from the surface, this will be a difficult task.

Overall, the here measured PLFA contents (4–122 ng/g) are in a similar range to nearby collected soil samples from another study (Shen, 2020). Furthermore, the PLFA diversity is lower compared to, for example, more humid sites near the coast (diversity of about 60 different PLFAs), but is in the range of samples from the Yungay area, where the PLFA diversity was 11 at 0–5 cm depth and 12 in 20–30 cm depth (Schulze-Makuch et al., 2018). Similarly, Shen (2020) found a PLFA diversity ranging from 7 to 15 individual PLFAs, along a North-South transect (22.3°S–28.4°S) with the lowest PLFA diversity of 7 in the Yungay area (~24°S). In this study, the PLFA diversity ranges from 5 to 16 different PLFAs highlighting that the local variability of samples only a few centimeters to <1 m apart is in the same range as the large-scale variability along a North-South transect (Shen, 2020). The slightly larger PLFA diversity in the surface units compared to the subsurface units might indicate an aeolian input of microorganisms to the surface (Figures 5, Figure 7), which is known for viable fungi and bacteria in the Atacama Desert (Azua-Bustos et al., 2019; Conley et al., 2006); whereas the subsurface should not directly be subject to airborne microorganisms. A decreasing microbial diversity with depth has also been observed for other alluvial deposits and playa sediments, which were associated with increasing salinity at deeper soil horizons (Fernández-Martínez et al., 2019; Warren-Rhodes et al., 2019).

In our study we show that polygonal networks represent habitable subsurface environments under transient moist conditions in the hyper-arid Atacama Desert. Hence, polygonal networks occurring in other hyper-arid environments such as on Mars might be relevant features for astrobiology. On Mars, polygonal networks occur, among other locations, in saline mid-Noachian to early Hesperian terrains of the Southern Highlands (Osterloo et al., 2008). These saline polygonal networks are associated with, among other processes, the past presence of water on early Mars and its evaporation (Ye et al., 2019). They might have been a potential microbial habitat, in which the polygons provided a higher water availability. Given the current absence of rain on Mars, the presence of hygroscopic salts and salts which contain crystal water suggests that Martian saline polygonal terrain could still represent a subsurface refuge today. Additionally, salts can enhance the stability of liquid water on Mars (Nair & Unnikrishnan, 2020), further promoting these features as sites with a high priority for sample return missions and/or as landing sites of exploratory rover missions (Ye et al., 2019).

5. Conclusion

A simulated rain event on a saline polygon and its adjacent salt-poor sand wedge in the Atacama Desert was conducted to investigate the effect of moistening on the local habitability conditions of the surface and near subsurface. Our study revealed the stimulation of microbial communities in the polygon subsurface sediments after soil wetting. Furthermore, it shows that in addition to moisture, also local soil heterogeneities, including polygon and sand wedge as well as heterogeneities at the intra-polygon and intra-sand wedge scale are likely to have a significant influence on the habitable conditions of these soils. Thus, the impact of such spatial soil heterogeneities on the abundance of the microbial signal partly masked small responses of the microbial community with respect to simulated changes in the water availability making the differentiation of natural and induced variation challenging. A better understanding of such small-scale abiotic soil heterogeneities is not only relevant for large-scale gradient studies assessing the habitability along climatic or precipitation gradients, but it also contributes to a better understanding of microbial habitats in hyper-arid settings on Earth and beyond.

Data Availability Statement

All raw data is now available at DepositOnce: <https://doi.org/10.14279/depositonce-16571>.

Acknowledgments

This project was supported by the Elsa-Neumann-Stipendium des Landes Berlin and Studienstiftung des deutschen Volkes. We would like to thank the Department of Applied Geochemistry and the Institute of Food Technology and Food Chemistry of the Technische Universität Berlin for the use of their facilities as well as Charlotte Stehle for her help during the project. Open Access funding enabled and organized by Projekt DEAL.

References

- Arens, F. L., Airo, A., Feige, J., Sager, C., Wiechert, U., & Schulze-Makuch, D. (2021). Geochemical proxies for water-soil interactions in the hyperarid Atacama Desert, Chile. *Catena*, 206, 105531. <https://doi.org/10.1016/j.catena.2021.105531>
- Azua-Bustos, A., González-Silva, C., & Fairén, A. G. (2022). The Atacama Desert in northern Chile as an analog model of Mars. *Frontiers in Astronomy and Space Sciences*, 8. <https://doi.org/10.3389/fspas.2021.810426>
- Azua-Bustos, A., González-Silva, C., Fernández-Martínez, M. Á., Arenas-Fajardo, C., Fonseca, R., Martín-Torres, F. J., et al. (2019). Aeolian transport of viable microbial life across the Atacama Desert, Chile: Implications for Mars. *Scientific Reports*, 9(1), 11024. <https://doi.org/10.1038/s41598-019-47394-z>
- Bligh, E. G., & Dyer, W. J. (1959). A rapid method of total lipid extraction and purification. *Canadian Journal of Biochemistry and Physiology*, 37(8), 911–917. <https://doi.org/10.1139/o59-099>
- Boy, D., Moeller, R., Sauheitl, L., Schaarschmidt, F., Rapp, S., van den Brink, L., et al. (2022). Gradient studies reveal the true drivers of extreme life in the Atacama Desert. *Journal of Geophysical Research: Biogeosciences*, 127(3), e2021JG006714. <https://doi.org/10.1029/2021JG006714>
- Carson, J. K., Campbell, L., Rooney, D., Clipson, N., & Gleeson, D. B. (2009). Minerals in soil select distinct bacterial communities in their microhabitats. *FEMS Microbiology Ecology*, 67(3), 381–388. <https://doi.org/10.1111/j.1574-6941.2008.00645.x>
- Certini, G., Campbell, C. D., & Edwards, A. C. (2004). Rock fragments in soil support a different microbial community from the fine Earth. *Soil Biology and Biochemistry*, 36(7), 1119–1128. <https://doi.org/10.1016/j.soilbio.2004.02.022>
- Conley, C. A., Ishkhanova, G., McKay, C. P., & Cullings, K. (2006). A preliminary survey of non-lichenized fungi cultured from the hyperarid Atacama Desert of Chile. *Astrobiology*, 6(4), 521–526. <https://doi.org/10.1089/ast.2006.6.521>
- Connon, S. A., Lester, E. D., Shafaat, H. S., Obenhuber, D. C., & Ponce, A. (2007). Bacterial diversity in hyperarid Atacama Desert soils. *Journal of Geophysical Research*, 112(G4), G04S17. <https://doi.org/10.1029/2006JG000311>
- Crits-Christoph, A., Robinson, C. K., Barnum, T., Fricke, W. F., Davila, A. F., Jedynek, B., et al. (2013). Colonization patterns of soil microbial communities in the Atacama Desert. *Microbiome*, 1(1), 28. <https://doi.org/10.1186/2049-2618-1-28>
- Davila, A. F., Hawes, I., Ascaso, C., & Wierzychos, J. (2013). Salt deliquescence drives photosynthesis in the hyperarid Atacama Desert. *Environmental Microbiology Reports*, 5(4), 583–587. <https://doi.org/10.1111/1758-2229.12050>
- Davila, A. F., & Schulze-Makuch, D. (2016). The last possible outposts for life on Mars. *Astrobiology*, 16(2), 159–168. <https://doi.org/10.1089/ast.2015.1380>
- Diaz, G. C. (1994). The nitrate deposits of Chile. In K.-J. Reutter, E. Scheuber, & P. J. Wigger (Eds.), *Tectonics of the southern central Andes* (pp. 303–316). Springer Berlin Heidelberg. https://doi.org/10.1007/978-3-642-77353-2_22
- Erickson, G. E. (1981). Geology and origin of the Chilean nitrate deposits. In *Professional Paper* (p. 1188). <https://doi.org/10.3133/pp1188>
- Erickson, G. E. (1983). The Chilean nitrate deposits: The origin of the Chilean nitrate deposits, which contain a unique group of saline minerals, has provoked lively discussion for more than 100 years. *American Scientist*, 71(4), 366–374. Retrieved from <http://www.jstor.org/stable/27852136>
- Ewing, S. A., Sutter, B., Owen, J., Nishiizumi, K., Sharp, W., Cliff, S. S., et al. (2006). A threshold in soil formation at Earth's arid-hyperarid transition. *Geochimica et Cosmochimica Acta*, 70(21), 5293–5322. <https://doi.org/10.1016/j.gca.2006.08.020>
- Fernández-Martínez, M. Á., dos Santos Severino, R., Moreno-Paz, M., Gallardo-Carreño, I., Blanco, Y., Warren-Rhodes, K. A., et al. (2019). Prokaryotic community structure and metabolisms in shallow subsurface of Atacama Desert Playas and alluvial fans after heavy rains: Repairing and preparing for next dry period. *Frontiers in Microbiology*, 10, 1641. <https://doi.org/10.3389/fmicb.2019.01641>
- Harvey, H., Fallon, R. D., & Patton, J. S. (1986). The effect of organic matter and oxygen on the degradation of bacterial membrane lipids in marine sediments. *Geochimica et Cosmochimica Acta*, 50(5), 795–804. [https://doi.org/10.1016/0016-7037\(86\)90355-8](https://doi.org/10.1016/0016-7037(86)90355-8)
- Houston, J. (2006). Variability of precipitation in the Atacama Desert: Its causes and hydrological impact. *International Journal of Climatology*, 26(15), 2181–2198. <https://doi.org/10.1002/joc.1359>
- Houston, J., & Hartley, A. J. (2003). The central Andean west-slope rainshadow and its potential contribution to the origin of hyper-aridity in the Atacama Desert. *International Journal of Climatology*, 23(12), 1453–1464. <https://doi.org/10.1002/joc.938>
- Huang, W., Ertekin, E., Wang, T., Cruz, L., Dailey, M., DiRuggiero, J., & Kisailus, D. (2020). Mechanism of water extraction from gypsum rock by desert colonizing microorganisms. *Proceedings of the National Academy of Sciences of the United States of America*, 117(20), 10681–10687. <https://doi.org/10.1073/pnas.2001613117>
- Hwang, Y., Schulze-Makuch, D., Arens, F. L., Saenz, J. S., Adam, P. S., Sager, C., et al. (2021). Leave no stone unturned: Individually adapted xerotolerant Thaumarchaeota sheltered below the boulders of the Atacama Desert hyperarid core. *Microbiome*, 9(1), 234. <https://doi.org/10.1186/s40168-021-01177-9>
- Jordan, T. E., Kirk-Lawlor, N. E., Blanco, N. P., Rech, J. A., & Cosentino, N. J. (2014). Landscape modification in response to repeated onset of hyperarid paleoclimate states since 14 Ma, Atacama Desert, Chile. *Geological Society of America Bulletin*, 126(7–8), 1016–1046. <https://doi.org/10.1130/B30978.1>
- Knief, C., Bol, R., Amelung, W., Kusch, S., Frindt, K., Eckmeier, E., et al. (2020). Tracing elevational changes in microbial life and organic carbon sources in soils of the Atacama Desert. *Global and Planetary Change*, 184, 103078. <https://doi.org/10.1016/j.gloplacha.2019.103078>
- Kusch, S., Jaeschke, A., Mörchen, R., & Rethemeyer, J. (2020). Tracing life at the dry limit using phospholipid fatty acids – Does sampling matter? *Soil Biology and Biochemistry*, 141, 107661. <https://doi.org/10.1016/j.soilbio.2019.107661>
- Lebron, I., Herrero, J., & Robinson, D. A. (2009). Determination of gypsum content in dryland soils exploiting the gypsum-bassanite phase change. *Soil Science Society of America Journal*, 73(2), 403–411. <https://doi.org/10.2136/sssaj2008.0001>
- Logemann, J., Graue, J., Köster, J., Engelen, B., Rullkötter, J., & Cypionka, H. (2011). A laboratory experiment of intact polar lipid degradation in sandy sediments. *Biogeosciences*, 8(9), 2547–2560. <https://doi.org/10.5194/bg-8-2547-2011>
- Mangelsdorf, K., Karger, C., & Zink, K.-G. (2019). Phospholipids as life markers in geological habitats. In H. Wilkes (Ed.), *Springer nature living reference biomedical and life sciences. Hydrocarbons, oils and lipids: Diversity, origin, Chemistry and fate* (pp. 1–29). Springer. https://doi.org/10.1007/978-3-319-54529-5_12-1
- Müller, K.-D., Husmann, H., & Nalik, H. P. (1990). A new and rapid method for the assay of bacterial fatty acids using high resolution capillary gas chromatography and trimethylsulfonium hydroxide. *Zentralblatt für Bakteriologie*, 274(2), 174–182. [https://doi.org/10.1016/S0934-8840\(11\)80100-3](https://doi.org/10.1016/S0934-8840(11)80100-3)

- Nair, C. P. R., & Unnikrishnan, V. (2020). Stability of the liquid water phase on Mars: A thermodynamic analysis considering martian atmospheric conditions and perchlorate brine solutions. *ACS Omega*, 5(16), 9391–9397. <https://doi.org/10.1021/acsomega.0c00444>
- Navarro-González, R., Rainey, F. A., Molina, P., Bagaley, D. R., Hollen, B. J., de La Rosa, J., et al. (2003). Mars-like soils in the Atacama Desert, Chile, and the dry limit of microbial life. *Science (New York, N.Y.)*, 302(5647), 1018–1021. <https://doi.org/10.1126/science.1089143>
- Osterloo, M. M., Hamilton, V. E., Bandfield, J. L., Glotch, T. D., Baldrige, A. M., Christensen, P. R., et al. (2008). Chloride-bearing materials in the southern highlands of Mars. *Science (New York, N.Y.)*, 319(5870), 1651–1654. <https://doi.org/10.1126/science.1150690>
- Pedregosa, F., Varoquaux, G., Gramfort, A., Michel, V., Thirion, B., Grisel, O., et al. (2011). Scikit-learn: Machine learning in python. *Journal of Machine Learning Research*, 12(85), 2825–2830. Retrieved from <http://jmlr.org/papers/v12/pedregosa11a.html>
- Pfeiffer, M., Morgan, A., Heimsath, A., Jordan, T., Howard, A., & Amundson, R. (2021). Century scale rainfall in the absolute Atacama Desert: Landscape response and implications for past and future rainfall. *Quaternary Science Reviews*, 254, 106797. <https://doi.org/10.1016/j.quascirev.2021.106797>
- Sager, C., Airo, A., Arens, F. L., & Schulze-Makuch, D. (2021). New type of sand wedge polygons in the salt cemented soils of the hyper-arid Atacama Desert. *Geomorphology*, 373, 107481. <https://doi.org/10.1016/j.geomorph.2020.107481>
- Sager, C., Airo, A., Arens, F. L., & Schulze-Makuch, D. (2022). Eolian erosion of polygons in the Atacama Desert as a proxy for hyper-arid environments on Earth and beyond. *Scientific Reports*, 12(1), 12394. <https://doi.org/10.1038/s41598-022-16404-y>
- Schulze-Makuch, D., Lipus, D., Arens, F. L., Bague, M., Bornemann, T. L. V., de Vera, J.-P., et al. (2021). Microbial hotspots in lithic microhabitats inferred from DNA fractionation and metagenomics in the Atacama Desert. *Microorganisms*, 9(5), 1038. <https://doi.org/10.3390/microorganisms9051038>
- Schulze-Makuch, D., Wagner, D., Kounaves, S. P., Mangelsdorf, K., Devine, K. G., de Vera, J.-P., et al. (2018). Transitory microbial habitat in the hyperarid Atacama Desert. *Proceedings of the National Academy of Sciences of the United States of America*, 115(11), 2670–2675. <https://doi.org/10.1073/pnas.1714341115>
- Shen, J. (2020). Phospholipid biomarkers in Mars-analogous soils of the Atacama Desert. *International Journal of Astrobiology*, 19(6), 505–514. <https://doi.org/10.1017/S1473550420000294>
- Steinle, L., Knittel, K., Felber, N., Casalino, C., de Lange, G., Tassarolo, C., et al. (2018). Life on the edge: Active microbial communities in the Kryos MgCl₂-brine basin at very low water activity. *The ISME Journal*, 12(6), 1414–1426. <https://doi.org/10.1038/s41396-018-0107-z>
- Stevenson, A., Hamill, P. G., O’Kane, C. J., Kminek, G., Rummel, J. D., Voytek, M. A., et al. (2017). *Aspergillus penicillioides* differentiation and cell division at 0.585 water activity. *Environmental Microbiology*, 19(2), 687–697. <https://doi.org/10.1111/1462-2920.13597>
- Suutari, M., & Laakso, S. (1994). Microbial fatty acids and thermal adaptation. *Critical Reviews in Microbiology*, 20(4), 285–328. <https://doi.org/10.3109/10408419409113560>
- Suzuki, K., Collins, M. D., Iijima, E., & Komagata, K. (1988). Chemotaxonomic characterization of a radiotolerant bacterium, *Arthrobacter radiotolerans*: Description of *Rubrobacter radiotolerans* gen. nov., comb. nov. *FEMS Microbiology Letters*, 52(1–2), 33–39. <https://doi.org/10.1111/j.1574-6968.1988.tb02568.x>
- Warren-Rhodes, K. A., Lee, K. C., Archer, S. D. J., Cabrol, N., Ng-Boyle, L., Wettergreen, D., et al. (2019). Subsurface microbial habitats in an extreme Desert Mars-analog environment. *Frontiers in Microbiology*, 10, 69. <https://doi.org/10.3389/fmicb.2019.00069>
- Warren-Rhodes, K. A., Rhodes, K. L., Pointing, S. B., Ewing, S. A., Lacap, D. C., Gómez-Silva, B., et al. (2006). Hypolithic cyanobacteria, dry limit of photosynthesis, and microbial ecology in the hyperarid Atacama Desert. *Microbial Ecology*, 52(3), 389–398. <https://doi.org/10.1007/s00248-006-9055-7>
- White, D. C., Davis, W. M., Nickels, J. S., King, J. D., & Bobbie, R. J. (1979). Determination of the sedimentary microbial biomass by extractable lipid phosphate. *Oecologia*, 40(1), 51–62. <https://doi.org/10.1007/BF00388810>
- Wierzchos, J., Artieda, O., Ascaso, C., Nieto García, F., Vitek, P., Azua-Bustos, A., & Fairén, A. G. (2020). Crystalline water in gypsum is unavailable for cyanobacteria in laboratory experiments and in natural desert endolithic habitats. *Proceedings of the National Academy of Sciences of the United States of America*, 117(45), 27786–27787. <https://doi.org/10.1073/pnas.2013134117>
- Wierzchos, J., Ascaso, C., & McKay, C. P. (2006). Endolithic cyanobacteria in halite rocks from the hyperarid core of the Atacama Desert. *Astrobiology*, 6(3), 415–422. <https://doi.org/10.1089/ast.2006.6.415>
- Wierzchos, J., Cámara, B., de Los Ríos, A., Davila, A. F., Sánchez Almazo, I. M., Artieda, O., et al. (2011). Microbial colonization of Ca-sulfate crusts in the hyperarid core of the Atacama Desert: Implications for the search for life on Mars. *Geobiology*, 9(1), 44–60. <https://doi.org/10.1111/j.1472-4669.2010.00254.x>
- Ye, B., Huang, J., Michalski, J., & Xiao, L. (2019). Geomorphologic characteristics of polygonal features on chloride-bearing deposits on Mars: Implications for martian hydrology and astrobiology. *Journal of Earth System Science*, 30(5), 1049–1058. <https://doi.org/10.1007/s12583-019-1212-2>
- Zhang, Z., Qu, Y., Li, S., Feng, K., Wang, S., Cai, W., et al. (2017). Soil bacterial quantification approaches coupling with relative abundances reflecting the changes of taxa. *Scientific Reports*, 7(1), 4837. <https://doi.org/10.1038/s41598-017-05260-w>
- Zinelabedin, A., Riedesel, S., Reimann, T., Ritter, B., & Dunai, T. J. (2022). Testing the potential of using coarse-grain feldspars for post-IR IRSL dating of calcium sulphate-wedge growth in the Atacama Desert. *Quaternary Geochronology*, 71, 101341. <https://doi.org/10.1016/j.quageo.2022.101341>
- Zink, K.-G., & Mangelsdorf, K. (2004). Efficient and rapid method for extraction of intact phospholipids from sediments combined with molecular structure elucidation using LC-ESI-MS-MS analysis. *Analytical and Bioanalytical Chemistry*, 380(5–6), 798–812. <https://doi.org/10.1007/s00216-004-2828-2>